7. Fritsche LG, Chen W, Schu M, et al. Seven new loci associated with age-related macular degeneration. *Nat Genet.* 2013;45: 433–439.

8. Tam PO, Ng TK, Liu DT, et al. HTRA1 variants in exudative age-related macular degeneration and interactions with smoking and CFH. *Invest Ophthalmol Vis Sci.* 2008;49:2357–2365.

9. Neale BM, Fagerness J, Reynolds R, et al. Genome-wide association study of advanced age-related macular degeneration identifies a role of the hepatic lipase gene (LIPC). *Proc Natl Acad Sci U S A.* 2010;107:7395–7400.

10. Dewan A, Liu M, Hartman S, et al. HTRA1 promoter polymorphism in wet age-related macular degeneration. *Science.* 2006;314:989–992.

11. Fuse N, Miyazawa A, Mengkegale M, et al. Polymorphisms in complement factor H and hemicentin-1 genes in a Japanese population with dry-type age-related macular degeneration. *Am J Ophthalmol.* 2006;142:1074–1076.

12. Gotoh N, Yamada R, Hiratani H, et al. No association between complement factor H gene polymorphism and exudative age-related macular degeneration in Japanese. *Hum Genet.* 2006; 120:139–143.

13. Grassi MA, Fingert JH, Scheetz TE, et al. Ethnic variation in AMD-associated complement factor H polymorphism p.Tyr402His. *Hum Mutat.* 2006;27:921–925.

14. Uka J, Tamura H, Kobayashi T, et al. No association of complement factor H gene polymorphism and age-related macular degeneration in the Japanese population. *Retina.* 2006;26:985–987.

15. Okamoto H, Umeda S, Obazawa M, et al. Complement factor H polymorphisms in Japanese population with age-related macular degeneration. *Mol Vis.* 2006;12:156–158.

16. Chen LJ, Liu DT, Tam PO, et al. Association of complement factor H polymorphisms with exudative age-related macular degeneration. *Mol Vis.* 2006;12:1536–1542.

17. Yoshida T, DeWan A, Zhang H, et al. HTRA1 promoter polymorphism predisposes Japanese to age-related macular degeneration. *Mol Vis.* 2007;13:545–548.

18. Yang Z, Camp NJ, Sun H, et al. A variant of the HTRA1 gene increases susceptibility to age-related macular degeneration. *Science.* 2006;314:992–993.

19. Fritsche LG, Loenhardt T, Janssen A, et al. Age-related macular degeneration is associated with an unstable ARMS2 (LOC387715) mRNA. *Nat Genet.* 2008;40:892–896.

20. Yang Z, Tong Z, Chen Y, et al. Genetic and functional dissection of HTRA1 and LOC387715 in age-related macular degeneration. *PLoS Genet.* 2010;6:e1000836.

21. Friedrich U, Myers CA, Fritsche LG, et al. Risk- and non-risk-associated variants at the 10q26 AMD locus influence ARMS2 mRNA expression but exclude pathogenic effects due to protein deficiency. *Hum Mol Genet.* 2011;20:1387–1399.

22. Kanda A, Stambolian D, Chen W, Curcio CA, Abecasis GR, Swaroop A. Age-related macular degeneration-associated variants at chromosome 10q26 do not significantly alter ARMS2 and HTRA1 transcript levels in the human retina. *Mol Vis.* 2010;16:1317–1323.

23. Kortvely E, Hauck SM, Duetsch G, et al. ARMS2 is a constituent of the extracellular matrix providing a link between familial and sporadic age-related macular degenerations. *Invest Ophthalmol Vis Sci.* 2010;51:79–88.

24. Wang G, Spencer KL, Court BL, et al. Localization of age-related macular degeneration-associated ARMS2 in cytosol, not mitochondria. *Invest Ophthalmol Vis Sci.* 2009;50:3084–3090.

25. Seddon JM, Willett WC, Speizer FE, Hankinson SE. A prospective study of cigarette smoking and age-related macular degeneration in women. *JAMA.* 1996;276:1141–1146.

26. Vingerling JR, Hofman A, Grobbee DE, de Jong PT. Age-related macular degeneration and smoking. The Rotterdam Study. *Arch Ophthalmol.* 1996;114:1193–1196.

27. DeAngelis MM, Ji F, Kim IK, et al. Cigarette smoking, CFH, APOE, ELOVL4, and risk of neovascular age-related macular degeneration. *Arch Ophthalmol.* 2007;125:49–54.

28. Oneill C, Jamison J, McCulloch D, Smith D. Age-related macular degeneration: cost-of-illness issues. *Drugs Aging.* 2001;18:233–241.

29. Fraser-Bell S, Wu J, Klein R, Azen SP, Varma R. Smoking, alcohol intake, estrogen use, and age-related macular degeneration in Latinos: the Los Angeles Latino Eye Study. *Am J Ophthalmol.* 2006;141:79–87.

30. Conley YP, Jakobsdottir J, Mah T, et al. CFH, ELOVL4, PLEKHA1 and LOC387715 genes and susceptibility to age-related maculopathy: AREDS and CHS cohorts and meta-analyses. *Hum Mol Genet.* 2006;15:3206–3218.

31. Smith W, Assink J, Klein R, et al. Risk factors for age-related macular degeneration: pooled findings from three continents. *Ophthalmology.* 2001;108:697–704.

32. Wang AL, Lukas TJ, Yuan M, Du N, Handa JT, Neufeld AH. Changes in retinal pigment epithelium related to cigarette smoke: possible relevance to smoking as a risk factor for age-related macular degeneration. *PLoS One.* 2009;4:e5304.

33. Schmidt S, Hauser MA, Scott WK, et al. Cigarette smoking strongly modifies the association of LOC387715 and age-related macular degeneration. *Am J Hum Genet.* 2006;78:852–864.

34. Fujihara M, Nagai N, Sussan TE, Biswal S, Handa JT. Chronic cigarette smoke causes oxidative damage and apoptosis to retinal pigmented epithelial cells in mice. *PLoS One.* 2008;3: e3119.

35. Espinosa-Heidmann DG, Suner IJ, Catanuto P, Hernandez EP, Marin-Castano ME, Cousins SW. Cigarette smoke-related oxidants and the development of sub-RPE deposits in an experimental animal model of dry AMD. *Invest Ophthalmol Vis Sci.* 2006;47:729–737.

36. Grau S, Richards PJ, Kerr B, et al. The role of human HtrA1 in arthritic disease. *J Biol Chem.* 2006;281:6124–6129.

37. Chamberland A, Wang E, Jones AR, et al. Identification of a novel HtrA1-susceptible cleavage site in human aggrecan: evidence for the involvement of HtrA1 in aggrecan proteolysis in vivo. *J Biol Chem.* 2009;284:27352–27359.

38. Shiga A, Nozaki H, Yokoseki A, et al. Cerebral small-vessel disease protein HTRA1 controls the amount of TGF-beta1 via cleavage of proTGF-beta1. *Hum Mol Genet.* 2011;20:1800–1810.

39. Clausen T, Southan C, Ehrmann M. The HtrA family of proteases: implications for protein composition and cell fate. *Mol Cell.* 2002;10:443–455.

40. Tocharus J, Tsuchiya A, Kajikawa M, Ueta Y, Oka C, Kawaichi M. Developmentally regulated expression of mouse HtrA3 and its role as an inhibitor of TGF-beta signaling. *Dev Growth Differ.* 2004;46:257–274.

41. Jones A, Kumar S, Zhang N, et al. Increased expression of multifunctional serine protease, HTRA1, in retinal pigment epithelium induces polypoidal choroidal vasculopathy in mice. *Proc Natl Acad Sci U S A.* 2011;108:14578–14583.

42. Yannuzzi LA, Sorenson J, Spaide RF, Lipson B. Idiopathic polypoidal choroidal vasculopathy (IPCV). 1990. *Retina.* 2012;32(suppl 1):1–8.

43. Nakashizuka H, Mitsumata M, Okisaka S, et al. Clinicopathologic findings in polypoidal choroidal vasculopathy. *Invest Ophthalmol Vis Sci.* 2008;49:4729–4737.

44. Witmer AN, Vrensen GF, Van Noorden CJ, Schlingemann RO. Vascular endothelial growth factors and angiogenesis in eye disease. *Prog Retin Eye Res.* 2003;22:1–29.

45. Smith CJ, Hansch C. The relative toxicity of compounds in mainstream cigarette smoke condensate. *Food Chem Toxicol.* 2000;38:637–646.

46. Clemons TE, Milton RC, Klein R, Seddon JM, Ferris FL III. Risk factors for the incidence of advanced age-related macular degeneration in the Age-Related Eye Disease Study (AREDS) AREDS report no. 19. *Ophthalmology.* 2005;112:533–539.

47. Klein R, Knudtson MD, Cruickshanks KJ, Klein BE. Further observations on the association between smoking and the long-term incidence and progression of age-related macular degeneration: the Beaver Dam Eye Study. *Arch Ophthalmol.* 2008;126:115–121.

48. Yang Z, Stratton C, Francis PJ, et al. Toll-like receptor 3 and geographic atrophy in age-related macular degeneration. *N Engl J Med.* 2008;359:1456–1463.

49. Dogusan Z, Garcia M, Flamez D, et al. Double-stranded RNA induces pancreatic beta-cell apoptosis by activation of the toll-like receptor 3 and interferon regulatory factor 3 pathways. *Diabetes.* 2008;57:1236–1245.

50. Seya T, Matsumoto M. The extrinsic RNA-sensing pathway for adjuvant immunotherapy of cancer. *Cancer Immunol Immunother.* 2009;58:1175–1184.

51. Kleinman ME, Kaneko H, Cho WG, et al. Short-interfering RNAs induce retinal degeneration via TLR3 and IRF3. *Mol Ther.* 2012;20:101–108.

ORIGINAL ARTICLE

The first *USH2A* mutation analysis of Japanese autosomal recessive retinitis pigmentosa patients: a totally different mutation profile with the lack of frequent mutations found in Caucasian patients

Yang Zhao[1,2], Katsuhiro Hosono[1], Kimiko Suto[1], Chie Ishigami[3], Yuuki Arai[4], Akiko Hikoya[1], Yasuhiko Hirami[4], Masafumi Ohtsubo[2], Shinji Ueno[5], Hiroko Terasaki[5], Miho Sato[1], Hiroshi Nakanishi[6], Shiori Endo[6], Kunihiro Mizuta[6], Hiroyuki Mineta[6], Mineo Kondo[7], Masayo Takahashi[3], Shinsei Minoshima[2] and Yoshihiro Hotta[1]

Retinitis pigmentosa (RP) is a highly heterogeneous genetic disease. The *USH2A* gene, which accounts for approximately 74–90% of Usher syndrome type 2 (USH2) cases, is also one of the major autosomal recessive RP (arRP) causative genes among Caucasian populations. To identify disease-causing *USH2A* gene mutations in Japanese RP patients, all 73 exons were screened for mutations by direct sequencing. In total, 100 unrelated Japanese RP patients with no systemic manifestations were identified, excluding families with obvious autosomal dominant inheritance. Of these 100 patients, 82 were included in this present study after 18 RP patients with very likely pathogenic *EYS* (eyes shut homolog) mutations were excluded. The mutation analysis of the *USH2A* revealed five very likely pathogenic mutations in four patients. A patient had only one very likely pathogenic mutation and the others had two of them. Caucasian frequent mutations p.C759F in arRP and p.E767fs in USH2 were not found. All the four patients exhibited typical clinical features of RP. The observed prevalence of *USH2A* gene mutations was approximately 4% among Japanese arRP patients, and the profile of the *USH2A* gene mutations differed largely between Japanese patients and previously reported Caucasian populations.

Journal of Human Genetics (2014) **59**, 521–528; doi:10.1038/jhg.2014.65; published online 31 July 2014

INTRODUCTION

Usher syndrome (USH; Mendelian inheritance in man (MIM) 276900) is an autosomal recessive disorder characterized by retinitis pigmentosa (RP) and hearing loss, with or without vestibular dysfunction. The syndrome is clinically and genetically heterogeneous and can be clinically classified into three subtypes on the basis of severity and progression of hearing loss and the presence or absence of vestibular dysfunction.[1] Specifically, USH type 2 (USH2), the most common type accounting for >50% of USH cases, is characterized by congenital mild-to-severe hearing loss and a normal vestibular response.[2] The *USH2A* (Usher syndrome 2A) gene, which encodes usherin, accounts for approximately 80% of USH2 cases.[3–5] Previous mutation analyses of the full-length *USH2A* coding region (exons 2–72) in Caucasian patients have revealed a frequent mutation c.2299delG (p.E767fs) in exon 13.[4–12] In our recent analysis of the

USH2A gene in Japanese USH2 patients, in which the p.E767fs mutation was not identified, we reported 19 novel mutations among 19 patients, as well as the splicing mutation c.8559-2A>G in 4 of the 19 patients, indicating that the incidence of mutations in the Japanese individuals was similar to that in Caucasian individuals, even though the mutation spectrum of the *USH2A* gene considerably differed between the two populations.[13–15]

RP (MIM 268000) is a highly heterogeneous genetic retinal degeneration characterized by night blindness and visual field constriction, which would eventually lead to severe visual impairment. The disease can be inherited via an autosomal recessive (ar), autosomal dominant (ad) or X-linked recessive mode or may occur in isolation; in fact, more than half of the cases in Japan are isolated cases.[16] To date, 63 causative genes and 7 loci have been found to be associated with RP (http://www.sph.uth.tmc.edu/Retnet/; accessed

[1]Department of Ophthalmology, Hamamatsu University School of Medicine, Hamamatsu, Japan; [2]Department of Photomedical Genomics, Basic Medical Photonics Laboratory, Medical Photonics Research Center, Hamamatsu University School of Medicine, Hamamatsu, Japan; [3]Laboratory for Retinal Regeneration, RIKEN Center for Developmental Biology, Kobe, Japan; [4]Department of Ophthalmology, Institute of Biomedical Research and Innovation Hospital, Kobe, Japan; [5]Department of Ophthalmology, Nagoya University Graduate School of Medicine, Nagoya, Japan; [6]Department of Otorhinolaryngology/Head and Neck Surgery, Hamamatsu University School of Medicine, Hamamatsu, Japan and [7]Department of Ophthalmology, Mie University Graduate School of Medicine, Tsu, Japan
Correspondence: Dr Y Hotta, Department of Ophthalmology, Hamamatsu University School of Medicine, 1-20-1 Handayama, Hamamatsu-shi, Higashi-ku, Shizuoka 431-3192, Japan.
E-mail: hotta@hama-med.ac.jp
Received 8 March 2014; revised 20 May 2014; accepted 3 July 2014; published online 31 July 2014

19 February 2014). The *EYS* (eyes shut homolog) gene encodes an ortholog of *Drosophila* spacemaker (spam), which is a protein essential for maintaining the photoreceptor morphology. *EYS* gene mutations have been detected in arRP-affected families of different ancestral origins and have been reported to account for 5–16% of arRP cases.[17–22] Mutations in the *USH2A* gene were also found to cause non-syndromic RP.[23] Although some studies on the *USH2A* gene employed mostly USH patients and included a few non-syndromic RP patients,[5,24,25] a few groups analyzed large sets of non-syndromic RP patients and reported that *USH2A* mutations, including the frequent mutation c.2276G>T (p.C759F), cause a substantial number of cases of non-syndromic RP in North America and Spain (7–23%).[23,26–29] We previously screened all *EYS* gene exons in 100 unrelated Japanese RP patients and, surprisingly, found *EYS* gene mutations in at least 18% of the arRP patients.[30] Of these 100 patients, 82 were included in the present study after 18 RP patients with very likely pathogenic (deleterious) *EYS* gene mutations were excluded.[30] Here we report the results of our study of all *USH2A* exons in 82 Japanese arRP patients.

MATERIALS AND METHODS

Patients

We previously screened all *EYS* gene exons in 100 unrelated Japanese RP patients with no systemic manifestations, excluding families with obvious autosomal dominant inheritance.[30] Among them, some pedigrees showed a pattern compatible with the recessive mode of inheritance, whereas other patients were considered as isolated cases. Excluding 18 RP patients with very likely pathogenic *EYS* gene mutations, 82 out of these 100 patients were employed in this study. An audiological examination, including pure-tone audiometry, was not performed before the mutation analysis; however, none of the patients had documented hearing loss. In addition, 200 unrelated and non-RP Japanese individuals were screened as controls to evaluate the frequency of mutations found in patient samples. Japanese patients with RP were examined at the Department of Ophthalmology, Hamamatsu University Hospital in Hamamatsu (by YH); the Department of Ophthalmology, Kobe City Medical Center General Hospital in Kobe (by MT); the Department of Ophthalmology, Institute of Biomedical Research and Innovation Hospital in Kobe (by MT); or the Department of Ophthalmology, Nagoya University Hospital in Nagoya (by MK and SU). These patients were from the areas of Tokyo to Osaka in Japan.

Ethics statements

This study was approved by the Institutional Review Board for Human Genetic and Genome Research at the four participating institutions (Hamamatsu University School of Medicine, RIKEN Center for Developmental Biology, Institute of Biomedical Research and Innovation Hospital and Nagoya University Graduate School of Medicine). All the procedures conformed to the tenets of the Declaration of Helsinki. Written informed consent was obtained from all participants before the molecular genetic studies were performed.

Mutation analysis

Genomic DNA extracted from peripheral lymphocytes of patients using standard procedures was amplified by PCR using the primer sets described in Supplementary Table S1. The PCR and sequencing procedures used were described previously.[30] A total of 73 exons, including a non-coding exon (exon 1) that covers the 5′ untranslated region, 71 coding exons (exons 2–72) and an alternatively spliced variant of exon 71,[31] were analyzed in both sense and antisense directions. Alternatively spliced exon 71 encodes a 24-amino-acid peptide in the murine inner ear and is considered to be well conserved in humans, even though its presence in human transcripts has not yet been directly confirmed. The accession numbers for the two alternative splicing isoforms (long isoform,[8] consisting of 72 exons, and longer isoform, consisting

of 73 exons that included an alternatively spliced variant of exon 71) of *USH2A* genes were NM_206933 (long isoform) and ENST00000366943 (longer isoform). The latter is the Ensembl Transcript ID number in the Ensembl database, which is presented here, because the entry of the longer isoform was not found in the DDBJ/EMBL/GenBank database.

Assessment of pathogenicity

A sequence variant was considered pathogenic when it represented a nonsense mutation, a frameshift mutation, a deletion mutation affecting amino-acid sequences, a mutation in the first two bases of canonical intron splice donor or acceptor sites, a missense mutation affecting a conserved amino-acid residue, a previously described pathogenic mutation or a mutation identified in >2 unrelated patients and did not appear in 200 unrelated and non-RP Japanese control samples or a public single-nucleotide polymorphism (SNP) database (NCBI dbSNP database, http://www.ncbi.nlm.nih.gov/projects/SNP/; 1000 Genomes database, http://www.1000genomes.org/). In particular, a missense mutation was described as very likely pathogenic when it fulfilled at least two of the following criteria: (1) it was found together with a second variant, especially a nonsense mutation or frameshift mutation; (2) it was segregated with the disease phenotype within the family; and (3) the *in silico* analysis predicted a pathogenic effect.

In silico analysis to assess the pathogenicity of a missense or deletion mutation

We used the five following computational algorithms to evaluate the pathogenicity of missense mutations: SIFT (http://sift.jcvi.org/www/SIFT_seq_submit2.html), PolyPhen2 (http://genetics.bwh.harvard.edu/pph2/), PMut (http://mmb.pcb.ub.es/PMut/), SNAP (http://rostlab.org/services/snap/), and Align-GVGD (http://agvgd.iarc.fr/agvgd_input.php). The SIFT analysis results are given by a probability of 0–1; specifically, mutations with a probability ≤0.05 are predicted to be deleterious (affect protein function), whereas those with a probability >0.05 are predicted to be tolerated. In this study, a mutation predicted to 'affect protein function' was considered as a suspected pathogenic mutation. Polyphen2 describes mutations as 'benign', 'possibly damaging' or 'probably damaging'. In this study, both 'possibly damaging' and 'probably damaging' were classified as suspected pathogenic mutations. The results from the SNAP analysis are classified into 'neutral' or 'non-neutral'. In this study, 'non-neutral' was considered as a suspected pathogenic mutation. The results from the PMut analysis are classified into 'neutral' or 'pathological'. In this study, 'pathological' was considered as a suspected pathogenic mutation. The Align-GVGD analysis results are given by a grade from C0 to C65, where C0 is benign and C65 is most likely pathogenic. In this study, a grade of C65 was considered as a suspected pathogenic mutation.

The secondary structure of usherin was predicted by PSIPRED v3.3 on the PSIPRED server (http://bioinf.cs.ucl.ac.uk/psipred/).

Clinical evaluation

The doctors were asked to obtain as much detail as possible about the family history of patients in whom we identified very likely pathogenic mutations (RP7H, RP10H, RP15H and RP66K) and possible pathogenic mutations (RP82K and RP85N). The complete history and medical records of these four patients were reviewed. In addition, patients were also clinically evaluated by standard procedures, including spectral-domain optical coherence tomography (Spectralis OCT; Heidelberg Engineering, Heidelberg, Germany or Cirrus OCT; Carl Zeiss Meditec, Inc., Dublin, CA, USA). Electroretinograms were also performed in some cases. Audiological examination, including pure-tone audiometry, was performed for patients (RP7H, RP10H and RP15H) who consented to the study.

RESULTS

Mutation analysis

Our mutation analysis of the *USH2A* gene in 82 unrelated Japanese patients revealed 5 very likely pathogenic mutations among 4 patients. A patient had only one very likely pathogenic mutation

Table 1 Mutation spectrum of the USH2A gene among Japanese families

Family ID	Nucleotide change	Predicted effect	Domain[a]	Location in gene	Type of change	Reference
Families with very likely pathogenic mutations						
RP7H[b]	c.685G>C/c.3595_3597delGAA	p.G229R/p.E1199del	LamGL/FN3	Exon 4/exon 17	Compound heterozygous	This study/this study
RP10H[c]	c.685G>C;c.2776C>T	p.G229R;p.R926C	LamGL;EGF_Lam	Exon 4;exon 13	Heterozygous;heterozygous	This study;this study
RP15H	c.8559-2A>G/c.8559-2A>G			Intron 42/intron 42	Homozygous	Nakanishi et al.,[13,15] Dai et al.[32]
RP66K	c.468-14G>A			Intron 2	Heterozygous	Le Guédard-Méreuze et al.[33]
Families with novel possible pathogenic mutations						
RP82K	c.7156G>T	p.V2386F	FN3	Exon 38	Heterozygous	This study
RP85N	c.14243C>T	p.S4748F	FN3	Exon 65	Heterozygous	This study

Nucleotide numbering reflects cDNA numbering with +1 corresponding to A of the ATG translation initiation codon in the reference sequence NM_206933, according to the nomenclature recommended by the Human Genome Variation Society (www.hgvs.org/mutnomen).
The initiation codon was designated as codon 1. None of these seven mutations were found in the Japanese control individuals.
[a]USH2A has a signal peptide, a laminin G-like domain (LamGL), a laminin N-terminal domain, a laminin-type EGF-like domain (EGF_Lam), a fibronectin type 3 domain (FN3), a laminin G domain, a transmembrane domain, and a PDZ-binding domain. See Figure 2.
[b]Segregation analysis was performed for the patient. See Figure 1a.
[c]No segregation analysis could be performed in this patient owing to difficulties in collecting samples from the patient's family. Therefore, it was not confirmed that two mutations were located on different chromosomes.

Table 2 Summary of very likely and possible pathogenic mutations identified in 82 Japanese patients with autosomal recessive retinitis pigmentosa

Nucleotide change	Predicted effect	Location in gene	Domain[a]	Conservation in H/B/D/R/M/C/Z[c]	Allele frequency Control frequency	Allele frequency Patient frequency	Family ID	Population	SIFT	PolyPhen2	PMut	SNAP	Align-GVGD
Very likely pathogenic mutations													
Splicing													
c.468-14G>A		Intron 2		Not applicable	0/400	1/164	RP66K	Japanese, French[33]					
c.8559-2A>G		Intron 42		Not applicable	0/400	2/164	RP15H	Japanese,[13,15] Chinese[32]					
Deletion													
c.3595_3597delGAA	p.E1199del	Exon 17	FN3	E/E/E/E/E/E/T	0/400	1/164	RP7H	Japanese					
Missense													
c.685G>C	p.G229R	Exon 4	LamGL	G/G/G/G/G/G/G	0/400	2/164	RP7H, RP10H	Japanese	Affect (score 0.00)	Probably damaging	Neutral	Non-neutral	C65
c.2776C>T	p.R926C	Exon 13	EGF_Lam	R/R/R/R/R/R/R	0/400	1/164	RP10H	Japanese	Affect (score 0.00)	Probably damaging	Neutral	Non-neutral	C65
Possible pathogenic mutations													
Missense													
c.7156G>T	p.V2386F	Exon 38	FN3	V/I/V/T/T/I/E	0/400	1/164	RP82K	Japanese	Affect (score 0.05)	Benign	Neutral	Non-neutral	C45
c.14243C>T	p.S4748F	Exon 65	FN3	S/A/S/S/S/S/S	0/400	1/164	RP85N	Japanese	Affect (score 0.01)	Probably damaging	Pathological	Non-neutral	C65

[a]USH2A has a signal peptide, a laminin G-like domain (LamGL), a laminin N-terminal domain, a laminin-type EGF-like domain (EGF_Lam), a fibronectin type 3 domain (FN3), a laminin G domain, a transmembrane domain and a PDZ-binding domain. See Figure 2.
[b]SIFT, PolyPhen2, PMut, SNAP and Align-GVGD were used to evaluate the pathogenicity of missense mutations. See Materials and methods. Suspected pathogenic mutations are shown in bold.
[c]H/B/D/R/M/C/Z denotes human/bovine/dog/rat/mouse/chicken/zebrafish USH2A orthologs, the sequences of which were selected from the DDBJ/EMBL/GenBank database. Accession numbers were NM_206933 (human), NM_001191425 (bovine), XM_545710 (dog), NM_001244757 (rat), NM_021408 (mouse), XM_419417 (chicken) and XM_692343 (zebrafish).

and the others had two of them (Tables 1 and 2). These very likely pathogenic mutations consisted of a deletion mutation, two splicing mutations and two missense mutations. In addition, we identified two possible pathogenic mutations in two individual patients (Tables 1 and 2).

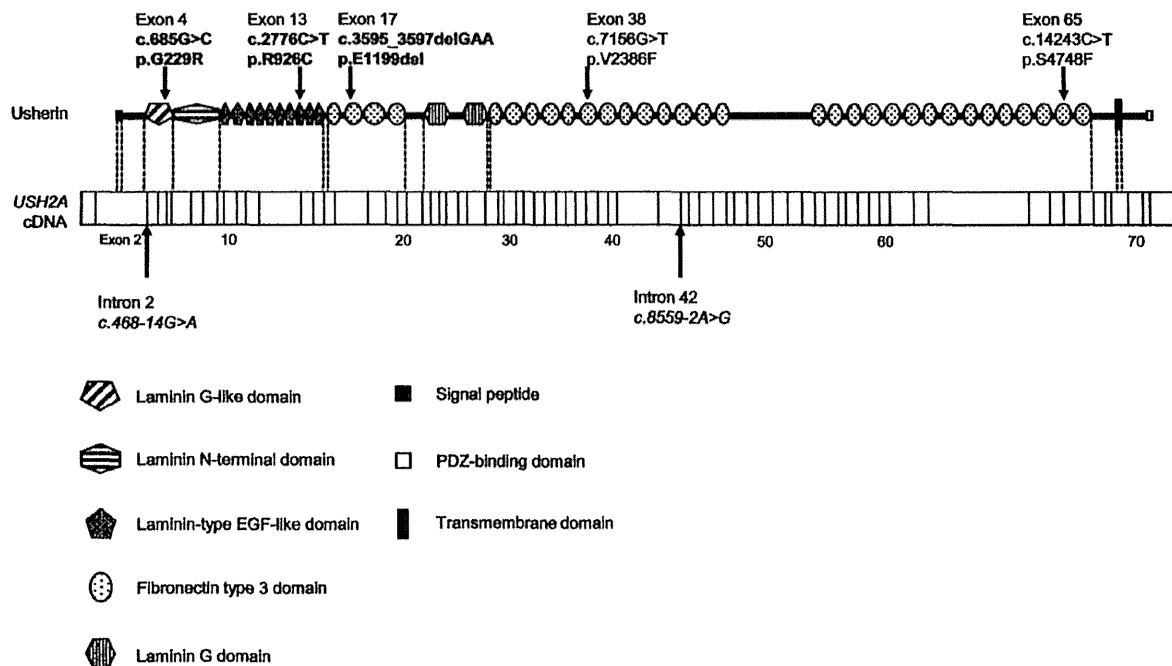### Families with very likely pathogenic mutations
Among the four patients carrying very likely pathogenic mutations, RP7H, RP10H and RP15H each had two pathogenic mutations. In RP7H and RP15H, the two mutated alleles were considered to be located on different chromosomes (Figures 1a and c).
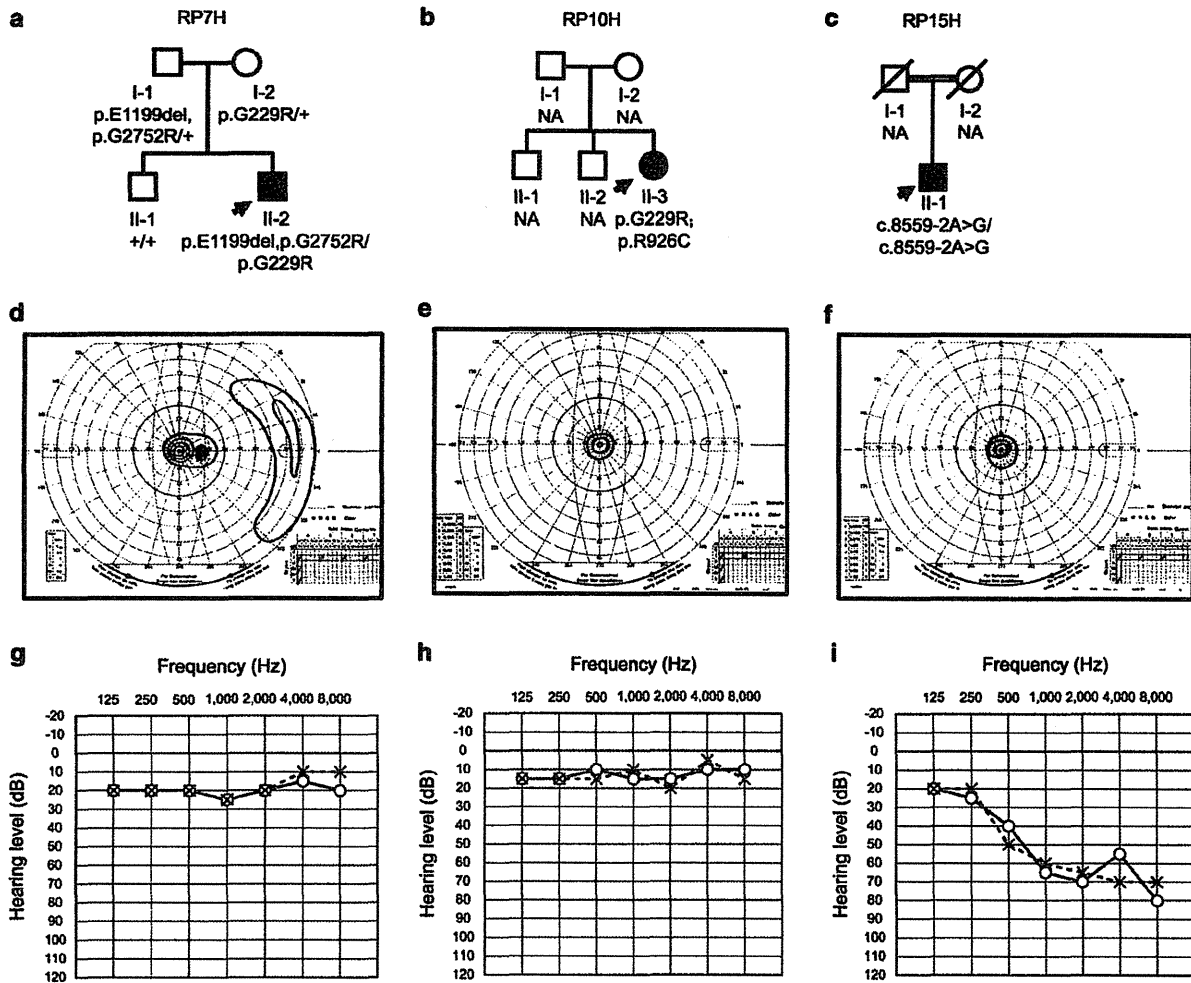
Figure 1 Pedigree and clinical examination data of patients with mutations in the *USH2A* gene. (a–c) Pedigrees of patients RP7H (a), RP10H (b) and RP15H (c). The genotypes are presented for p.E1199del, p.G229R, p.G2752R, p.R926C and c.8559-2A>G. The genotype of each evaluated individual is indicated below the symbol: square boxes and circles denote male and female individuals, respectively; black symbols indicate affected individuals; and slashed symbols indicate deceased individuals. The probands are indicated with arrows. NA, unavailable DNA samples. For example, c.8559-2A>G/ c.8559-2A>G, homozygous mutation carriers; p.G229R/+, heterozygous carriers; +/+, individuals carrying two wild-type alleles; p.E1199del/p.G229R, individuals who were compound heterozygous for both mutations. p.G229R;p.R926C could not be segregated (See Table 1 footnote). (d–f) Right visual fields of patients RP7H (d), RP10H (e) and RP15H (f). The constriction of visual fields was found to be symmetric. The concentric constriction started in their twenties or thirties, and no effective residual visual field was observed after their fifties. (g–i) Audiograms of patients RP7H (g), RP10H (h) and RP15H (i). Circles and crosses indicate hearing thresholds of the right and left ears, respectively.

Patient RP7H was born in the Hamamatsu area and was considered as an isolated case (Figure 1a). In RP7H, the proband (II-2) was compound heterozygous for the novel missense mutation c.685G>C (p.G229R) and the novel deletion mutation c.3595_3597delGAA (p.E1199del) (Figure 1a). p.G229R was also identified in patient RP10H, who was unrelated to RP7H (Tables 1 and 2). The amino-acid residue at G229 of human USH2A was compared with those encoded by the orthologous genes of some vertebrates (bovine, dog, rat, mouse, chicken and zebrafish) and was found to be highly conserved across species (Table 2). p.G229R was predicted to be pathogenic by four different computational prediction programs (SIFT, Polyphen2, SNAP and Align-GVGD). On the other hand, p.E1199del is a 3-base pair (bp) in-frame deletion that results in the

loss of the amino-acid residue E1199 in the second fibronectin type 3 domain (Figure 2). E1199 was also compared with the equivalent residue in other species' orthologous genes and was highly conserved among mammals and chicken (Table 2). p.E1199del was analyzed by the PSIPRED program to determine its effect on the secondary structure of usherin. The predicted effect was the shortening of the beta-sheet stretch from seven contiguous amino acids (QPCVSYE-1199) to five (QPCVS-1197), which suggests that the mutation affected the normal protein structure and was pathogenic. Interestingly, we also found another missense mutation c.8254G>A (p.G2752R), which we previously found in USH2 patient C212 as one of thee candidates for probable pathogenic mutations, but we could not determine the pathogenicity because of difficulty in the

Figure 2 Schematic distribution of the *USH2A* mutations identified in this study. Upper, usherin domains encoded by *USH2A*; lower, *USH2A* cDNA with exon boundaries. Novel very likely pathogenic mutations, novel possible pathogenic mutations and previously described mutations are shown in bold, normal and italic fonts, respectively. Identified mutations were widely distributed throughout almost the entire *USH2A* gene without any clear hot spot.

segregation analysis.[13] However, in this study, p.G2752R was assigned to the group of possible non-pathogenic sequence alterations (Supplementary Table S2), because it has been described in the dbSNP database (rs201863550) and the 1000 Genomes database. As shown in Figure 1a, the mutations were found to co-segregate with the disease phenotype as follows. The unaffected father (I-1) and mother (I-2) were heterozygous for p.E1199del and p.G229R, respectively, whereas the unaffected brother (II-1) carried the wild-type alleles. In addition, p.G2752R was identified in *cis* to p.E1199del in the unaffected father, indicating that these two mutations were genetically linked in this family.

Patient RP10H was born in the Hamamatsu area and was considered to be an isolated case (Figure 1b). RP10H was hetero-zygous for two missense mutations, c.685G>C (p.G229R) and c.2776C>T (p.R926C). p.G229R, also found in RP7H, was classified as very likely pathogenic as described above. Similarly, the novel missense mutation p.R926C was predicted to be pathogenic by four different computational prediction programs (SIFT, Polyphen2, SNAP and Align-GVGD) (Table 2). Like G229, the R926 residue was also found to be highly conserved across species (Table 2). No segregation analysis could be performed in this patient owing to difficulties in collecting samples from the patient's family. Although both these two missense mutations were considered pathogenic, we were not able to confirm whether they were located on different chromosomes (Figure 1b, Table 1).

Patient RP15H carried the homozygous c.8559-2A>G mutation; RP15H was an isolated case and his parents were second cousins from the Hamamatsu area; that is, he was the product of a consanguineous marriage (Figure 1c). The proband (II-1) was homozygous for the splicing mutation c.8559-2A>G. No segregation analysis was performed, because

both parents were deceased. Although the mutation has been previously reported as disease causing in four Japanese and one Chinese USH2 patients,[13,15,32] all of these five patients were heterozygous for c.8559-2A>G. To the best of our knowledge, this study is the first to report of a patient homozygous for the c.8559-2A>G mutation.

Patient RP66K was born in Kobe and was considered as an isolated case. In RP66K, we found the splicing mutation, c468-14G>A, which has been previously reported as disease causing in a French USH2 patient and shown to create a new AG (acceptor consensus) sequence, resulting in abnormal splicing.[33]

None of these five very likely pathogenic mutations was found among the Japanese controls or in a public SNP database (Table 2).

Families with novel possible pathogenic mutations

Here we report two novel missense mutations in two different patients (RP82K and RP85N), none of which was identified in 400 Japanese control alleles or a public SNP database. Patients RP82K and RP85N were born in the Kansai and Hiroshima areas, respectively, and were considered as isolated cases. RP82K and RP85N each had one novel missense mutation (p.V2386F and p.S4748F, respectively; Tables 1 and 2). The amino-acid residues of USH2A affected by the two novel missense mutations (V2386 and S4748) are not evolutionally conserved compared with those encoded by the orthologous genes of some vertebrate species (Table 2). For pathogenicity, the *in silico* analysis with at least two of the five different computational programs described these two mutations as pathogenic but did not exclude the possibility that these mutations were non-pathogenic (Table 2). Nevertheless, these two mutations were assigned to the group of possible

pathogenic mutations, and further analyses are necessary to determine the precise nature of these mutations.

Summary of the possible non-pathogenic sequence alterations in the USH2A gene identified in this study

Overall, 78 possible sequence alterations were identified among 82 patients, and 7 of them have never been reported (Supplementary Table S2). These alterations did not fulfill the assessment of pathogenicity in this study (See Materials and methods); therefore, they were assigned to the group of possible non-pathogenic sequence alterations (Supplementary Table S2).

Clinical findings

The age of the four patients with one or two deleterious mutations ranged from 19 to 52 years at the time of diagnosis and from 37 to 60 years at the time of initial examination for this study. In addition, all the four patients had night blindness. The constriction of visual fields was found to be symmetric. The concentric constriction started in their twenties or thirties, and no effective residual visual field was observed after their fifties (Figures 1d–f). In all cases, the fundus displayed changes typical of RP, including attenuated retinal vessels and bone spicule deposits over 360° of the fundus, all of which were increased in density with age. Spectral-domain OCT images also showed a marked reduction in retinal thickness resulting from the loss of photoreceptor layers. The photoreceptor inner segment/outer segment junction was either completely absent or was only detectable at the fovea of four subjects. The electroretinographic responses were consistent with severe generalized rod-cone dysfunction. On the other hand, none of these four patients had difficulties in daily conversation. Although the hearing tests for RP7H and RP10H yielded normal results (Figures 1g and h), the test for RP15H showed moderate hearing loss, suggesting USH2 (Figure 1i).

The age of the two patients with one possible mutation (RP82K and RP85N) was 40–46 years at the time of diagnosis and 50–66 years at the time of the initial examination for this study. Both patients had night blindness. The ocular findings including visual field, fundus, OCT and electroretinogram were compatible with the ocular findings in four patients with one or two deleterious mutations. Audiological examination, including pure-tone audiometry, was not performed, because the patients did not consent to the study.

DISCUSSION

This study is the first to analyze mutations in the USH2A gene among Japanese arRP patients with no systemic manifestations. In total, we detected 85 USH2A sequence alterations, of which 12 were novel. Among these 85 sequence alterations, 5 were classified as very likely pathogenic mutations (1 deletion, 2 splicing and 2 missense mutations), 2 were possibly pathogenic mutations (2 missense mutations) and 78 were possible non-pathogenic sequence alterations (Tables 1 and 2, and Supplementary Table S2). Among the 7 very likely and possible pathogenic mutations, a deletion and 4 missense mutations were novel, whereas the other 2 splicing mutations have been reported as disease causing in USH2 patients.[13,15,32,33] Similar to our previous study of Japanese USH2 patients, our current study did not detect the most prevalent mutations, p.E767fs and p.C759F, which account for approximately 23–39% and 1–14% of mutated alleles, respectively, in Caucasian individuals.[7–11] These results indicate that the profile of USH2A gene mutations differs largely between Japanese patients and previously reported Caucasian populations.[4–12,23,24,26–29]

We previously screened all EYS gene exons in 100 unrelated Japanese arRP patients with no systemic manifestations, with the exclusion of families showing obvious autosomal dominant inheritance, and, as a result, detected EYS gene mutations in 18–26% of the patients.[30] Excluding 18 RP patients with very likely pathogenic EYS gene mutations, 82 of these 100 patients were employed in this study. Among them, we found at least one very likely pathogenic or possible pathogenic USH2A gene mutation in six cases, of which three had two mutations and three had one mutation (Tables 1 and 2). Previous studies reported that 23 out of the 96 USH2 patients carried heterozygous USH2A gene mutations,[5] implying that this finding could be due to relatively large heterozygous deletions or deep intronic mutations.[34] In this study, because the direct sequences of PCR-amplified samples were used, we were not able to detect large deletions, insertions or rearrangements. In addition, because audiograms were not obtained from all patients with USH2A gene mutations, some of them may be USH2 patients without documented hearing loss. Therefore our results can only provide an estimate of the prevalence of USH2A mutations among Japanese arRP patients without documented systemic manifestations, including hearing loss. Considering only one or two deleterious mutations, the minimum observed prevalence of distinct USH2A gene mutations is 4% (4/100). If the patients with one heterogeneous possible pathogenic mutation are included in the estimation, the prevalence increases to 6% (6/100). A few previous studies on USH2A mutations employed large sets of non-syndromic RP patients, which accounted for 7–23% of arRP patients.[23,26–29] A possible reason for why the estimated prevalence in our study was lower than that of previous reports may be the fact that the Japanese population does not carry the p.E767fs or p.C759F mutation.

A previous report employing Japanese USH2 patients detected the c.8559-2A>G mutation in 4 out of the 19 cases, suggesting a possible frequent USH2A gene mutation among the Japanese population.[13,15] Here we identified that RP15H was homozygous for the c.8559-2A>G mutation, supporting the possibility of a frequent USH2A gene mutation among the Japanese population. To the best of our knowledge, this study is the first to report a patient homozygous for the c.8559-2A>G mutation. Although RP15H did not have documented hearing loss or communication problems, the hearing test demonstrated that the patient had moderate sensorineural hearing loss. A detailed medical interview revealed that the patient, a 61-year-old male, noticed a slight difficulty in hearing but considered it as age-appropriate. Elderly subjects, especially those aged >60 years, are affected by age-related hearing deterioration that makes it difficult to distinguish hearing loss from age-appropriate hearing. Therefore, auditory examination, including pure-tone audiometry, may be recommended for accurate evaluation of auditory function in elderly subjects. However, in our opinion, we could determine the presence or absence of hearing loss and select RP patients without auditory examination, because most of the subjects included in this study were middle-aged or younger.

In RP85N, we also found another missense mutation, c.2802T>G (p.C934W), which was previously reported as disease causing in a Chinese RP patient without hearing loss, although it has also been identified in two Chinese individuals among 100 normal Chinese controls.[25] p.C934W was also listed in the dbSNP database (rs201527662) and the 1000 Genomes database and was detected in 1 of the 400 control alleles in this study. Therefore we evaluated p.C934W as a possible non-pathogenic sequence alteration in this study (Supplementary Table S2).

In our previous report, we were unable to assign three sequence alterations (p.C691T, p.G2752R and p.T3747R) identified in patient C212 or determine which one of them was pathogenic.[13] In this study, we found that RP7H was heterozygous for p.G2752R, which was absent from 400 control alleles. However, because p.G2752R was described in the public SNP database (rs201863550) and was found to be genetically linked to the 3-bp in-frame deletion mutation p.E1199del in the patient's family (Figure 1a), it was assigned to the group of possible non-pathogenic sequence alterations. We speculate that patient C212 may be compound heterozygous for p.C691T and p.T3747R.

Studies have reported the phenotype of non-syndromic RP caused by USH2A gene mutations among the Caucasian.[35] The patients in this present study shared a relatively uniform phenotype, characterized by a symptom-free interval in the first and second decades of life, followed by a rapid decline in visual functions due to concentric constriction. The four patients with one or two deleterious mutations did not have any documented hearing loss or pronunciation problems. Although the hearing test results for RP7H and RP10H were normal (Figures 1g and h), the results for RP15H showed moderate hearing loss, indicating USH2 (Figure 1i). These findings suggest that RP without documented hearing loss occasionally includes moderate type of USH2.

In conclusion, the profile of USH2A gene mutations in arRP patients with no systemic manifestations differs largely between Japanese and Caucasian. Considering only one or two deleterious mutations, the observed prevalence of distinct USH2A gene mutations among Japanese arRP patients with no systemic manifestations was 4% (4/100). Based on these data, if both EYS and USH2A genes are analyzed among Japanese arRP patients with no systemic manifestations, gene defects could be detected in 22–32% of the patients in total (18–26% and 4–6%, respectively). We believe that screening for these two genes is effective for genetic testing and counseling of RP patients in Japan.

CONFLICT OF INTEREST

The authors declare no conflict of interest.

1 Yan, D. & Liu, X. Z. Genetics and pathological mechanisms of Usher syndrome. J. Hum. Genet. 55, 327–335 (2010).

2 Rosenberg, T., Haim, M., Hauch, A. M. & Parving, A. The prevalence of Usher syndrome and other retinal dystrophy-hearing impairment associations. Clin. Genet. 51, 314–321 (1997).

3 Eudy, J. D., Weston, M. D., Yao, S., Hoover, D. M., Rehm, H. L., Ma-Edmonds, M. et al. Mutation of a gene encoding a protein with extracellular matrix motifs in Usher syndrome type IIa. Science 280, 1753–1757 (1998).

4 Weston, M. D., Eudy, J. D., Fujita, S., Yao, S., Usami, S., Cremers, C. et al. Genomic structure and identification of novel mutations in usherin, the gene responsible for Usher syndrome type IIa. Am. J. Hum. Genet. 66, 1199–1210 (2000).

5 Le Quesne Stabej, P., Saihan, Z., Rangesh, N., Steele-Stallard, H. B., Ambrose, J., Coffey, A. et al. Comprehensive sequence analysis of nine Usher syndrome genes in the UK National Collaborative Usher Study. J. Med. Genet. 49, 27–36 (2012).

6 Dreyer, B., Tranebjaerg, L., Brox, V., Rosenberg, T., Möller, C., Beneyto, M. et al. A common ancestral origin of the frequent and widespread 2299delG USH2A mutation. Am. J. Hum. Genet. 69, 228–234 (2001).

7 Bernal, S., Medà, C., Solans, T., Ayuso, C., Garcia-Sandoval, B., Valverde, D. et al. Clinical and genetic studies in Spanish patients with Usher syndrome type II: description of new mutations and evidence for a lack of genotype-phenotype correlation. Clin. Genet. 68, 204–214 (2005).

8 Aller, E., Jaijo, T., Beneyto, M., Nájera, C., Oltra, S., Ayuso, C. et al. Identification of 14 novel mutations in the long isoform of USH2A in Spanish patients with Usher syndrome type II. J. Med. Genet. 43, e55 (2006).

9 Baux, D., Larrieu, L., Blanchet, C., Hamel, C., Ben Salah, S., Vielle, A. et al. Molecular and in silico analyses of the full-length isoform of usherin identify new pathogenic alleles in Usher type II patients. Hum. Mutat. 28, 781–789 (2007).

10 Dreyer, B., Brox, V., Tranebjaerg, L., Rosenberg, T., Sadeghi, A. M., Möller, C. et al. Spectrum of USH2A mutations in Scandinavian patients with Usher syndrome type II. Hum. Mutat. 29, 451 (2008).

11 Yan, D., Ouyang, X., Patterson, D. M., Du, L. L., Jacobson, S. G. & Liu, X. Z. Mutation analysis in the long isoform of USH2A in American patients with Usher syndrome type II. J. Hum. Genet. 54, 732–738 (2009).

12 Aller, E., Larrieu, L., Jaijo, T., Baux, D., Espinós, C., González-Candelas, F. et al. The USH2A c.2299delG mutation: dating its common origin in a Southern European population. Eur. J. Hum. Genet. 18, 788–793 (2010).

13 Nakanishi, H., Ohtsubo, M., Iwasaki, S., Hotta, Y., Mizuta, K., Mineta, H. et al. Identification of 11 novel mutations in USH2A among Japanese patients with Usher syndrome type 2. Clin. Genet. 76, 383–391 (2009).

14 Nakanishi, H., Ohtsubo, M., Iwasaki, S., Hotta, Y., Mizuta, K., Mineta, H. et al. Hair roots as an mRNA source for mutation analysis of Usher syndrome-causing genes. J. Hum. Genet. 55, 701–703 (2010).

15 Nakanishi, H., Ohtsubo, M., Iwasaki, S., Hotta, Y., Usami, S., Mizuta, K. et al. Novel USH2A mutations in Japanese Usher syndrome type 2 patients: marked differences in the mutation spectrum between the Japanese and other populations. J. Hum. Genet. 56, 484–490 (2011).

16 Hayakawa, M., Fujiki, K., Kanai, A., Matsumura, M., Honda, Y., Sakaue, H. et al. Multicenter genetic study of retinitis pigmentosa in Japan: I. Genetic heterogeneity in typical retinitis pigmentosa. Jpn J. Ophthalmol. 41, 1–6 (1997).

17 Abd El-Aziz, M. M., Barragán, I., O'Driscoll, C. A., Goodstadt, L., Prigmore, E., Borrego, S. et al. EYS, encoding an ortholog of Drosophila spacemaker, is mutated in autosomal recessive retinitis pigmentosa. Nat. Genet. 40, 1285–1287 (2008).

18 Collin, R. W., Littink, K. W., Klevering, B. J., van den Born, L. I., Koenekoop, R. K., Zonneveld, M. N. et al. Identification of a 2 Mb human ortholog of Drosophila eyes shut/spacemaker that is mutated in patients with retinitis pigmentosa. Am. J. Hum. Genet. 83, 594–603 (2008).

19 Abd El-Aziz, M. M., O'Driscoll, C. A., Kaye, R. S., Barragán, I., El-Ashry, M. F., Borrego, S. et al. Identification of novel mutations in the ortholog of Drosophila eyes shut gene (EYS) causing autosomal recessive retinitis pigmentosa. Invest. Ophthalmol. Vis. Sci. 51, 4266–4272 (2010).

20 Audo, I., Sahel, J. A., Mohand-Saïd, S., Lancelot, M. E., Antonio, A., Moskova-Doumanova, V. et al. EYS is a major gene for rod-cone dystrophies in France. Hum. Mutat. 31, E1406–E1435 (2010).

21 Barragán, I., Borrego, S., Pieras, J. I., González-del Pozo, M., Santoyo, J., Ayuso, C. et al. Mutation spectrum of EYS in Spanish patients with autosomal recessive retinitis pigmentosa. Hum. Mutat. 31, E1772–E1800 (2010).

22 Littink, K. W., van den Born, L. I., Koenekoop, R. K., Collin, R. W., Zonneveld, M. N., Blokland, E. A. et al. Mutations in the EYS gene account for approximately 5% of autosomal recessive retinitis pigmentosa and cause a fairly homogeneous phenotype. Ophthalmology 117, 2026–2033 (2010).

23 Rivolta, C., Sweklo, E. A., Berson, E. L. & Dryja, T. P. Missense mutation in the USH2A gene: association with recessive retinitis pigmentosa without hearing loss. Am. J. Hum. Genet. 66, 1975–1978 (2000).

24 Aller, E., Nájera, C., Millán, J. M., Oltra, J. S., Pérez-Garrigues, H., Vilela, C. et al. Genetic analysis of 2299delG and C759F mutations (USH2A) in patients with visual and/or auditory impairments. Eur. J. Hum. Genet. 12, 407–410 (2004).

25 Xu, W., Dai, H., Lu, T., Zhang, X., Dong, B. & Li, Y. Seven novel mutations in the long isoform of the USH2A gene in Chinese families with non-syndromic retinitis pigmentosa and Usher syndrome Type II. Mol. Vis. 17, 1537–1552 (2011).

26 Bernal, S., Ayuso, C., Antiñolo, G., Gimenez, A., Borrego, S., Trujillo, M. J. et al. Mutations in USH2A in Spanish patients with autosomal recessive retinitis pigmentosa: high prevalence and phenotypic variation. J. Med. Genet. 40, e8 (2003).

27 Seyedahmadi, B. J., Rivolta, C., Keene, J. A., Berson, E. L. & Dryja, T. P. Comprehensive screening of the USH2A gene in Usher syndrome type II and non-syndromic recessive retinitis pigmentosa. Exp. Eye Res. 79, 167–173 (2004).

28 McGee, T. L., Seyedahmadi, B. J., Sweeney, M. O., Dryja, T. P. & Berson, E. L. Novel mutations in the long isoform of the USH2A gene in patients with Usher syndrome type II or non-syndromic retinitis pigmentosa. J. Med. Genet. 47, 499–506 (2010).

29 Ávila-Fernández, A., Cantalapiedra, D., Aller, E., Vallespín, E., Aguirre-Lambán, J., Blanco-Kelly, F. et al. Mutation analysis of 272 Spanish families affected by autosomal recessive retinitis pigmentosa using a genotyping microarray. Mol. Vis. 16, 2550–2558 (2010).

30 Hosono, K., Ishigami, C., Takahashi, M., Park, D. H., Hirami, Y., Nakanishi, H. et al. Two novel mutations in the EYS gene are possible major causes of autosomal recessive retinitis pigmentosa in the Japanese population. PLoS ONE 7, e31036 (2012).

31 Adato, A., Lefèvre, G., Delprat, B., Michel, V., Michalski, N., Chardenoux, S. et al. Usherin, the defective protein in Usher syndrome type IIA, is likely to be a component

of interstereocilia ankle links in the inner ear sensory cells. *Hum. Mol. Genet.* **14**, 3921–3932 (2005).

32 Dai, H., Zhang, X., Zhao, X., Deng, T., Dong, B., Wang, J. *et al*. Identification of five novel mutations in the long isoform of the *USH2A* gene in Chinese families with Usher syndrome type II. *Mol. Vis.* **14**, 2067–2075 (2008).

33 Le Guédard-Méreuze, S., Vaché, C., Baux, D., Faugère, V., Larrieu, L., Abadie, C. *et al*. Ex vivo splicing assays of mutations at noncanonical positions of splice sites in USHER genes. *Hum. Mutat.* **31**, 347–355 (2010).

34 Steele-Stallard, H. B., Le Quesne Stabej, P., Lenassi, E., Luxon, L. M., Claustres, M., Roux, A. F. *et al*. Screening for duplications, deletions and a common intronic mutation detects 35% of second mutations in patients with *USH2A* monoallelic mutations on Sanger sequencing. *Orphanet. J. Rare Dis.* **8**, 122 (2013).

35 Sandberg, M. A., Rosner, B., Weigel-DiFranco, C., McGee, T. L., Dryja, T. P. & Berson, E. L. Disease course in patients with autosomal recessive retinitis pigmentosa due to the *USH2A* gene. *Invest. Ophthalmol. Vis. Sci.* **49**, 5532–5539 (2008).

Supplementary Information accompanies the paper on Journal of Human Genetics website (http://www.nature.com/jhg)

CLINICAL INVESTIGATION

Autoantibodies to transient receptor potential cation channel, subfamily M, member 1 in a Japanese patient with melanoma-associated retinopathy

Yukiko Morita · Kazuhiro Kimura ·
Youichiro Fujitsu · Atsushi Enomoto ·
Shinji Ueno · Mineo Kondo · Koh-Hei Sonoda

Abstract

Purpose To report a case of melanoma-associated retinopathy (MAR) in a Japanese patient found to have autoantibodies to transient receptor potential cation channel, subfamily M, member 1 (TRPM1).

Case An 82-year-old man presented with blurred vision OS as well as night blindness and photopsia OU. Fundus photography, fluorescein angiography, and spectral domain-optical coherence tomography findings were essentially normal. Goldmann perimetry revealed a relative central scotoma, including the blind spot in the right eye, as well as a relative scotoma around a blind spot OS. The full-field scotopic electroretinograms showed a "negative-type" pattern OU, suggestive of extensive bipolar cell dysfunction. Systemic examination revealed that the patient had malignant melanoma of the anus with lung metastasis. Autoantibodies to TRPM1 were detected in the serum of the patient by immunoblot analysis. Vitreous opacity developed during follow-up. The visual symptoms and vitreous opacity of the patient were markedly improved after oral prednisolone therapy. The patient died as a result of widespread metastasis of the melanoma at 11 months after his first visit.

Conclusion The present case is the first reported instance of MAR positive for autoantibodies to TRPM1 in an Asian patient.

Keywords Melanoma-associated retinopathy · Electroretinogram (ERG) · Transient receptor potential cation channel, subfamily M, member 1 (TRPM1) · Paraneoplastic retinopathy

Introduction

Melanoma-associated retinopathy (MAR) is a paraneoplastic autoimmune manifestation of melanoma that is characterized by various visual signs and symptoms including night blindness, photopsia, visual field defects, and abnormal color vision [1–8]. Patients with MAR also have characteristic electroretinograms (ERGs). The scotopic full-field ERG elicited by a bright flash stimulus shows a "negative-type" pattern with an a-wave of normal amplitude and a b-wave smaller than the a-wave [1–6], suggesting that in MAR patients, the retinal bipolar cells are affected. Historically, autoantibodies to bipolar cells have been recognized as markers of MAR, but the specific bipolar cell antigen has not been identified [8–12].

We and others recently identified autoantibodies specific for transient receptor potential cation channel, subfamily M, member 1 (TRPM1) in the serum of MAR patients [13, 14]. TRPM1 is specifically expressed in retinal ON bipolar cells and functions as a component of the transduction channel in these cells [15–17]. All four MAR

Y. Morita · K. Kimura (✉) · Y. Fujitsu · K.-H. Sonoda
Department of Ophthalmology, Yamaguchi University Graduate
School of Medicine, 1-1-1 Minami-Kogushi, Ube,
Yamaguchi 755-8505, Japan
e-mail: k.kimura@yamaguchi-u.ac.jp

A. Enomoto
Department of Pathology, Nagoya University Graduate School
of Medicine, Nagoya, Japan

S. Ueno
Department of Ophthalmology, Nagoya University Graduate
School of Medicine, Nagoya, Japan

M. Kondo
Department of Ophthalmology, Mie University Graduate School
of Medicine, Tsu, Japan

patients with autoantibodies to TRPM1 in these previous reports were Caucasian [13, 14], and individuals with TRPM1-related MAR have not been described for other ethnic groups. Malignant melanoma is rare in the Japanese population, with a prevalence of only 0.002 %, compared with a frequency of 0.015 % in white populations.

We now report a case of MAR positive for serum autoantibodies to TRPM1 in a Japanese individual with melanoma of the anus and metastasis to the lung.

Case report

An 82-year-old man visited Yamaguchi University Hospital with complaints of blurred vision OS as well as night blindness and photopsia OU with a duration of about 1 month. He had not recently been diagnosed with any ocular or systemic disease, including any malignant tumors. His family history revealed no members with any eye diseases. Our initial examination found that his best corrected visual acuity (BCVA) was 1.2 OD and 0.6 OS. Slit-lamp assessment, intraocular pressure measurement, fundus examination, and fluorescein angiography findings were essentially normal OU (Fig. 1a, b). Spectral domain-optical coherence tomography (SD-OCT) (Cirrus HD-OCT; Carl Zeiss Meditec, Dublin, CA, USA) revealed a normal macular structure, with the exception of a slight irregularity of the retinal pigment epithelium in both eyes (Fig. 1c). The thickness of the parafoveal nasal inner nuclear layer (INL) was 40 μm OD and 36 μm OS. Given that the normal thickness of the parafoveal nasal INL was previously determined to be ~40 μm [18], there did not appear to be any thinning of the INL in this patient.

Goldmann perimetry revealed that the visual fields manifested general depression OU. A relative central scotoma including a blind spot was detected OD, and a relative scotoma around the blind spot was detected OS, with the I-4e target (Fig. 2a). Color vision tested with Ishihara color plates was normal, but the Standard Pseudoisochromatic Plates part 2 (SPP-2) test and the panel D-15 test revealed a mild blue-yellow defect OS. A dark-adaptation test revealed a poorly defined red-cone break and elevated threshold level, with a log threshold (arbitrary units) value of 6 after 40 min. Full-field ERGs were recorded with a bright flash stimulus of 20 J after 20 min of dark adaptation. They showed a normal a-wave and a b-wave with a markedly reduced amplitude, giving rise to a "negative-type" pattern OU (Fig. 2b).

On the basis of these ophthalmological and electrophysiological findings, we tentatively diagnosed the patient with paraneoplastic retinopathy and performed systemic examinations. Whole-body computed tomography (CT) revealed a tumor in his right lung (Fig. 2c). Biopsy

specimens were obtained from a hilar lymph node in the right lung by bronchoscopy, and histology revealed the mass to be a malignant melanoma (Fig. 2d). Positron emission tomography was performed, but the site of the primary tumor was not identified. There was physiological accumulation of the tracer in the bladder. We consulted a dermatologist, and the patient was then treated with DAV-Feron (dacarbazine, nimustine hydrochloride, vincristine, and interferon-β) chemotherapy. His BCVA remained at 1.0 OD and 0.7 OS, but vitreous opacity appeared OS and perimetry revealed enlarged blind spots OU.

Given that autoantibodies to TRPM1 have been detected in patients with paraneoplastic retinopathy associated with dysfunction of retinal ON bipolar cells [13, 14], we examined whether such autoantibodies were also present in the serum of our MAR patient. Immunoblot analysis revealed that serum from the patient yielded a pronounced immunoreactive band with lysates of cells transfected with an expression vector for human TRPM1 (Fig. 3). Negative control serum did not show such reactivity. These results suggested that the serum of the proband contained autoantibodies to TRPM1.

The patient received oral prednisolone at 40 mg/day for treatment of his MAR. Four weeks after the onset of prednisolone therapy, the vitreous opacity had disappeared and the blind spot enlargement was markedly attenuated OU. Four months after his initial visit, the patient was diagnosed with anal malignant melanoma, with the late diagnosis being attributable to the misidentification of his anal tumor as a hemorrhoid. The lung tumor was thus likely a metastasis from anal malignant melanoma. The patient died at 11 months after his first visit as a result of metastasis to the brain, lung, liver, bilateral hilar lymph nodes, mediastinal lymph nodes, and inguinal lymph nodes.

Discussion

The patient presented with blurred vision, night blindness, and photopsia associated with a "negative-type" ERG, indicative of dysfunction of retinal bipolar cells. Systemic examination revealed malignant melanoma in the lung and anus. The serum of the patient was also positive for autoantibodies to TRPM1. On the basis of these findings, we diagnosed the patient with MAR likely caused by autoantibodies to TRPM1. Only four patients with TRPM1-related MAR have been reported to date, all of whom were Caucasian [13, 14]. The present Japanese patient thus represents the first case of TRPM1-related MAR in an ethnic group other than Caucasian. Our findings suggest that autoantibodies to TRPM1 may play an important role in the pathogenesis of MAR regardless of ethnicity.
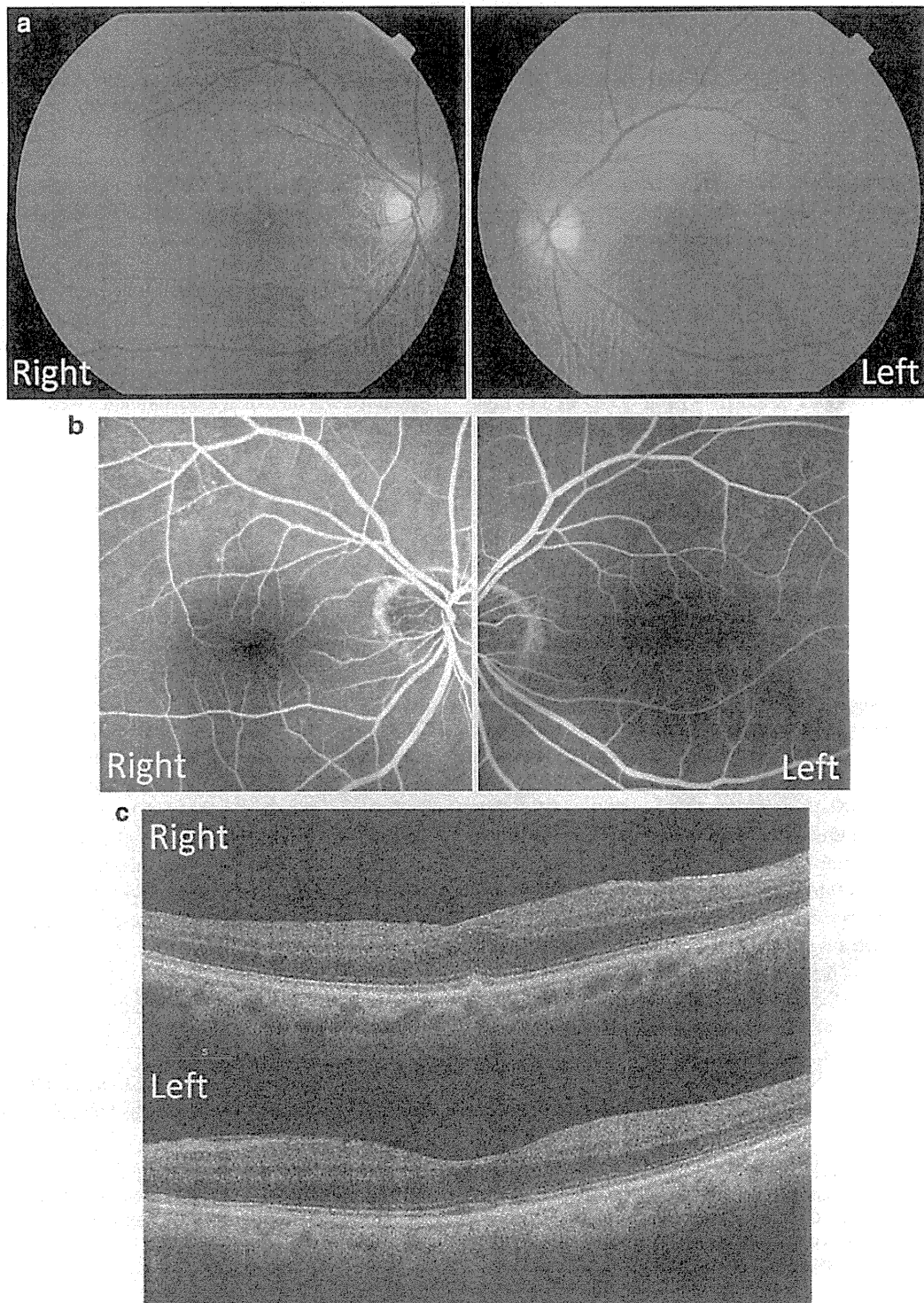
Fig. 1 Fundus photography, fluorescein angiography, and SD-OCT performed at the initial visit of the patient. **a** Fundus photographs revealed no abnormality in either eye. **b** Fundus fluorescence angiography revealed no abnormality in either eye. **c** Spectral domain-optical coherence tomography (SD-OCT) images for a 6-mm horizontal scan of the retina were essentially normal, with the exception of a slight irregularity of the retinal pigment epithelium in both eyes
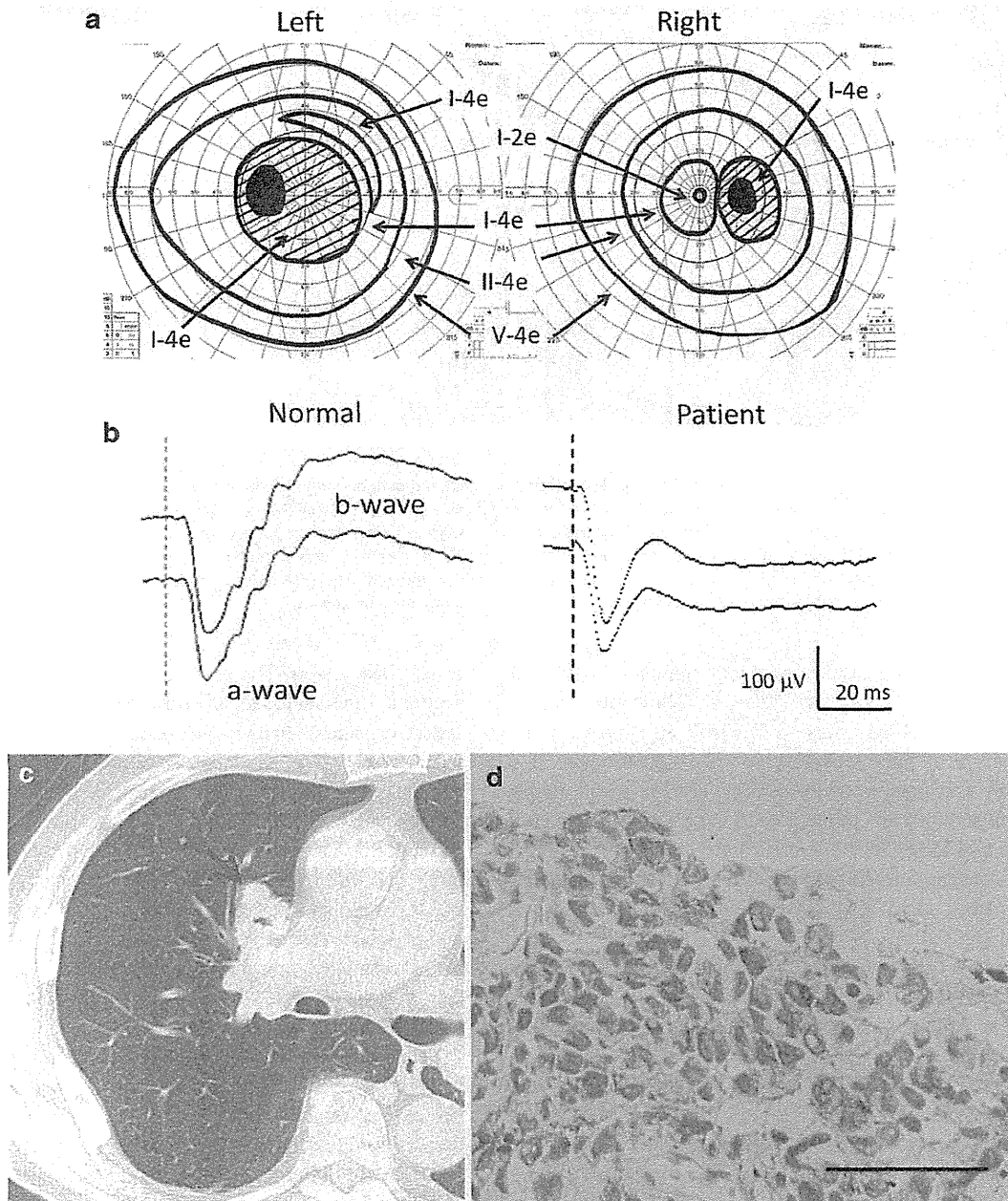
Fig. 2 Goldmann visual fields, full-field ERGs, CT of the right lung, and histology of a specimen obtained from the hilar lymph node of the patient. a Goldmann visual fields revealed a relative central scotoma including the blind spot OD and a relative scotoma around the blind spot OS. b Full-field electroretinograms (ERGs) with a bright flash stimulus after dark adaptation showed a "negative-type" pattern for the patient (*right*) compared with the normal pattern (*left*). c A computed tomography (CT) scan revealed a tumor in the right lung (*red arrow*). d Hematoxylin–eosin staining of a biopsy specimen obtained from a hilar lymph node in the right lung revealed spindle-shaped malignant cells. *Scale bar* 50 μm

TRPM1 is a component of the visual transduction cation channel specifically expressed in retinal ON bipolar cells [15–17, 19]. Immunohistology of the adult mouse retina revealed punctate TRPM1 signals at the tips of ON bipolar cell dendrites detected with antibodies to metabotropic glutamate receptor 6 (mGluR6) and to the α subunit of the G$_o$ protein [16]. TRPM1-null mice were also shown to lack ON bipolar cell responses to light [15, 16]. In addition, *TRPM1* mutations have been associated with the complete form of congenital stationary night blindness (CSNB) in
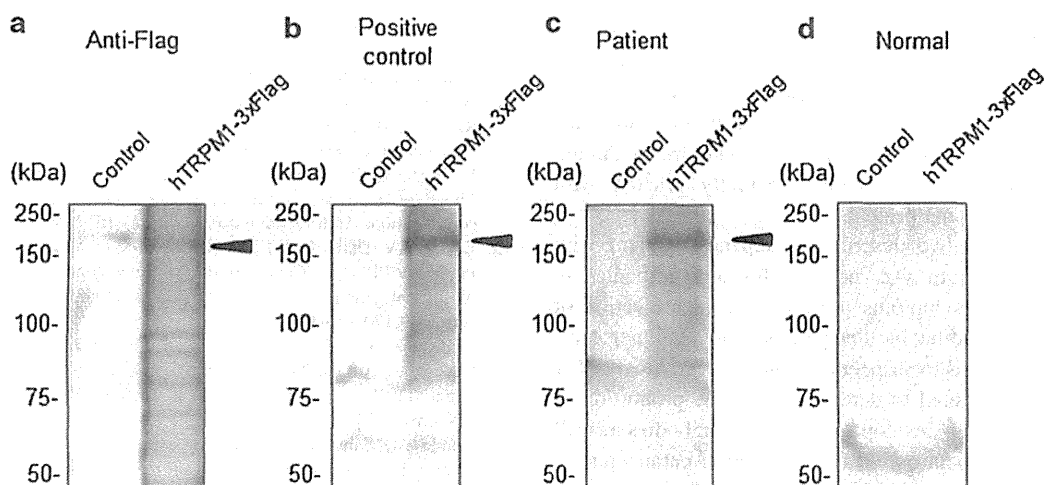
Fig. 3 Immunoblot analysis of serum from the patient for reactivity with TRPM1. HEK293T cells transfected with the expression vector pCAGGS alone (*control*) or with pCAGGS encoding human transient receptor potential cation channel, subfamily M, member 1 (*TRPM1*) tagged with three copies of the flag epitope were subjected to immunoblot analysis with antibodies to the flag tag (a), with serum from a patient previously shown to contain autoantibodies to TRPM1 as a positive control (b), with serum from the proband (c), and with normal control serum (d). *Arrowheads* indicate the 3× flag-tagged TRPM1 protein, which showed substantial reactivity with serum from the proband. The positions of molecular size standards (in kilodaltons) are also shown

humans, which is characterized by pronounced dysfunction of the retinal ON pathway [20–23]. These observations suggest that TRPM1 plays a key role in synaptic transmission from photoreceptors to ON bipolar cells. It is possible that ectopic expression of TRPM1 in the malignant melanoma cells of the patient triggered the production of autoantibodies to this protein by B lymphocytes. These antibodies might then have reacted with TRPM1 in retinal ON bipolar cells, resulting in severe dysfunction of the retinal ON pathway.

The average latency from the diagnosis of melanoma to that of MAR was previously found to be 3.6 years, with a range of 2 months–19 years [5]. We diagnosed the present patient with malignant melanoma after only 18 days from the time of his first visit. However, he died 11 months later as a result of metastasis to several organs. In the present case, the visual symptoms preceded the diagnosis of malignant melanoma. The patient complained of blurred vision, night blindness, and photopsia; but Fundus photographs, fluorescein angiograms, and SD-OCT findings were all essentially normal at his initial visit. Perimetry revealed relative scotomas OU. It was his "negative-type" ERGs, indicative of extensive bipolar cell dysfunction, that led us to suspect the patient might have MAR. We, therefore, recommend that ERGs be performed on patients with progressive visual disturbance of unknown origin.

"Negative-type" ERGs are also observed in patients with CSNB. A previous study [5] found that 18 of 27 patients with MAR showed either central or paracentral scotomas or depressions, and 6 of 27 patients had arcuate visual field defects. The present patient had relative central scotomas that included or surrounded the blind spot. In contrast, patients with CSNB manifest a largely intact visual field. MAR patients also show a greater loss of S (blue) cone sensitivity by perimetry than do CSNB patients, and S cone ERGs were not detected in MAR patients [2]. Two subtypes of CAR were previously identified [2]: one in which cone cells are damaged and in which Goldmann perimetry reveals central scotoma, and one in which rod cells are damaged and in which Goldmann perimetry reveals annular scotoma. We speculate that the visual field disturbance of the present patient reflected damage to cone cells.

Drug therapy for MAR is aimed at immunomodulation in order to attenuate the autoimmune attack on the retina before irreversible damage occurs. Treatments include corticosteroid administration, plasmapheresis, intravenous injection of immunoglobulin and immunosuppression. However, the effectiveness of these treatments remains unclear. Oral corticosteroid treatment alone was found to be beneficial in only one of seven patients [5]. In the present study, the patient was treated with oral prednisolone. We believe that this treatment was effective because the vitreous opacity and enlarged blind spots were markedly attenuated after its onset. Further studies are needed to determine the optimal treatment for MAR.

There are several limitations to our study. First, we recorded only bright-flash ERGs after dark adaptation; we did not record rod responses to low-intensity stimuli, photopic responses, or photopic ERGs in response to a

long-duration stimulus in order to determine whether the postreceptor ON pathway was specifically affected. Second, we did not perform immunohistochemical analysis with the serum of the patient to confirm that the autoantibodies recognize retinal bipolar cells. And third, we did not confirm that the autoantibodies actually reacted with malignant melanoma proteins.

In conclusion, we described a Japanese patient with MAR whose serum was positive for autoantibodies to TRPM1. Visual symptoms preceded the identification of malignant melanoma in this patient, and his "negative-type" ERGs led us to suspect a diagnosis of MAR. Further studies are warranted to determine both the proportion of MAR patients who develop TRPM1 autoantibodies as well as the best treatment option for this type of paraneoplastic retinopathy.

References

1. Berson EL, Lessell S. Paraneoplastic night blindness with malignant melanoma. Am J Ophthalmol. 1988;106:307–11.

2. Milam AH, Saari JC, Jacobson SG, Lubinski WP, Feun LG, Alexander KR. Autoantibodies against retinal bipolar cells in cutaneous melanoma-associated retinopathy. Invest Ophthalmol Vis Sci. 1993;34:91–100.

3. Potter MJ, Thirkill CE, Dam OM, Lee AS, Milam AH. Clinical and immunocytochemical findings in a case of melanoma-associated retinopathy. Ophthalmology. 1999;106:2121–5.

4. Lei B, Bush RA, Milam AH, Sieving PA. Human melanoma-associated retinopathy (MAR) antibodies alter the retinal ON response of the monkey ERG in vivo. Invest Ophthalmol Vis Sci. 2000;41:262–6.

5. Keltner JL, Thirkill CE, Yip PT. Clinical and immunologic characteristics of melanoma-associated retinopathy syndrome: eleven new cases and a review of 51 previously published cases. J Neuroophthalmol. 2001;21:173–87.

6. Alexander KR, Barnes CS, Fishman GA, Milam AH. Nature of the cone ON pathway dysfunction in melanoma-associated retinopathy. Invest Ophthalmol Vis Sci. 2002;43:1189–97.

7. Chan JW. Paraneoplastic retinopathies and optic neuropathies. Surv Ophthalmol. 2003;48:12–38.

8. Adamus G. Autoantibody targets and their cancer relationship in the pathogenicity of paraneoplastic retinopathy. Autoimmun Rev. 2009;8:410–4.

9. Potter MJ, Adamus G, Szabo SM, Lee R, Mohaseb K, Behn D. Autoantibodies to transducin in a patient with melanoma-associated retinopathy. Am J Ophthalmol. 2002;134:128–30.

10. Hartmann TB, Bazhin AV, Schadendorf D, Eichmuller SB. SEREX identification of new tumor antigens linked to melanoma-associated retinopathy. Int J Cancer. 2005;114:88–93.

11. Lu Y, Jia L, He S, Hurley MC, Leys MJ, Jayasundera T, et al. Melanoma-associated retinopathy: a paraneoplastic autoimmune complication. Arch Ophthalmol. 2009;127:1572–80.

12. Bazhin AV, Dalke C, Willner N, Abschütz O, Wildberger HGH, Philippov PP, et al. Cancer-retina antigens as potential paraneoplastic antigens in melanoma-associated retinopathy. Int J Cancer. 2009;124:140–9.

13. Dhingra A, Fina ME, Neinstein A, Ramsey DJ, Xu Y, Fishman GA, et al. Autoantibodies in melanoma-associated retinopathy target TRPM1 cation channels of retinal ON bipolar cells. J Neurosci. 2011;31:3962–7.

14. Kondo M, Sanuki R, Ueno S, Nishizawa Y, Hashimoto N, Ohguro H, et al. Identification of autoantibodies against TRPM1 in patients with paraneoplastic retinopathy associated with ON bipolar cell dysfunction. PLoS One. 2011;6:e19911.

15. Morgans CW, Zhang J, Jeffrey BG, Nelson SM, Burke NS, Duvoisin RM, et al. TRPM1 is required for the depolarizing light response in retinal ON bipolar cells. Proc Natl Acad Sci USA. 2009;106:19174–8.

16. Koike C, Obara T, Uriu Y, Numata T, Sanuki R, Miyata K, et al. TRPM1 is a component of the retinal ON bipolar cell transduction channel in the mGluR6 cascade. Proc Natl Acad Sci USA. 2010;107:332–7.

17. Koike C, Numata T, Ueda H, Mori Y, Furukawa T. TRPM1: a vertebrate TRP channel responsible for retinal ON bipolar function. Cell Calcium. 2010;48:95–101.

18. Loduca AL, Zhang C, Zelkha R, Shahidi M. Thickness mapping of retinal layers by spectral-domain optical coherence tomography. Am J Ophthalmol. 2010;150:849–55.

19. Klooster J, Blokker J, Ten Brink JB, Unmehopa U, Fluiter K, Bergen AA. Ultrastructural localization and expression of TRPM1 in the human retina. Invest Ophthalmol Vis Sci. 2011;52:8356–62.

20. Li Z, Sergouniotis PI, Michaelides M, Mackay DS, Wright GA, Devery S, et al. Recessive mutations of the gene TRPM1 abrogate ON bipolar cell function and cause complete congenital stationary night blindness in humans. Am J Hum Genet. 2009;85:711–9.

21. van Genderen MM, Bijveld MM, Claassen YB, Florijn RJ, Pearring JN, Meire FM, et al. Mutations in TRPM1 are a common cause of complete congenital stationary night blindness. Am J Hum Genet. 2009;85:730–6.

22. Audo I, Kohl S, Leroy BP, Munier FL, Guillonneau X, Mohand-Saïd S, et al. TRPM1 is mutated in patients with autosomal-recessive complete congenital stationary night blindness. Am J Hum Genet. 2009;85:720–9.

23. Nakamura M, Sanuki R, Yasuma TR, Onishi A, Nishiguchi KM, Koike C, et al. TRPM1 mutations are associated with the complete form of congenital stationary night blindness. Mol Vis. 2010;16:425–37.

Changes in Outer Retinal Microstructures during Six Month Period in Eyes with Acute Zonal Occult Outer Retinopathy-Complex

CrossMark

Yoshitsugu Matsui[1], Hisashi Matsubara[1], Shinji Ueno[2], Yasuki Ito[2], Hiroko Terasaki[2], Mineo Kondo[1]*

1 Department of Ophthalmology, Mie University Graduate School of Medicine, Tsu, Japan, 2 Department of Ophthalmology, Nagoya University Graduate School of Medicine, Nagoya, Japan

Abstract

Purpose: To study the changes in the outer retinal microstructures during a six month period after the onset of acute zonal occult outer retinopathy (AZOOR)-complex by spectral-domain optical coherence tomography (SD-OCT).

Methods: Seventeen eyes of 17 patients with the AZOOR-complex were studied. The integrity of the external limiting membrane (ELM), ellipsoid zone (EZ; also called the inner/outer segment junction), and interdigitation zone (IDZ; also called the cone outer segment tips) were evaluated in the SD-OCT images obtained at the initial visit and at six months. The three highly reflective bands were divided into three types; continuous, discontinuous, and absent. The integrity of the outer nuclear layer (ONL) was also assessed.

Results: Among the three highly reflective bands, the IDZ was most altered at the initial visit and least recovered at six months. Fifteen of 17 eyes (88%) had a recovery of at least one of the three bands at six months in the retinal area where the ONL was intact, and these areas showed an improvement of visual field. Three eyes (18%) had retinal areas where the ONL was absent at the initial visit, and there was no recovery in both the retinal structures and visual fields in these areas.

Conclusions: Our results indicate that more than 85% eyes with AZOOR-complex show some recovery in the microstructures of the outer retina during a six month period if the ONL is intact. We conclude that SD-OCT is a useful method to monitor the changes of the outer retinal microstructure in eyes with the AZOOR-complex.

Introduction

Acute zonal occult outer retinopathy (AZOOR) is a retinal disease that was first reported by Gass [1]. AZOOR is characterized by an acute loss of one or more zones of outer retinal function, photopsia, minimal funduscopic changes, and electroretinographic (ERG) abnormalities [1–4]. AZOOR occurs predominantly in young women, and some patients have a viral-like illness before the onset [1,4,5]. The exact pathogenesis of AZOOR is still uncertain, but two possible hypotheses have been advanced; virus infection of the photoreceptors [6] and common genetic hypothesis of autoimmune/inflammatory disease [7].

In 2003, Gass suggested that retinal diseases similar to AZOOR, e.g., multiple evanescent white dot syndrome (MEWDS), multifocal choroiditis and panuveitis (MFP), punctate inner choroidopathy (PIC), acute idiopathic blind spot enlargement (AIBSE), acute macular neuroretinopathy (AMN), and AZOOR, were part of a spectrum of a single disease with similar clinical signs, symptoms, and ophthalmological findings [6]. He recommended that these should be placed in a single clinical entity

called the AZOOR-complex. There are several studies that reported that two of these diseases can occur in the same patient at the same time or at different times [8–12].

Optical coherence tomography (OCT) is a useful method to detect subtle morphological changes in retinas affected by various pathological conditions. Past studies have demonstrated the diagnostic value of time-domain (TD) and spectral-domain (SD) OCT in eyes with AZOOR-complex. The findings showed that the integrity of the external limiting membrane (ELM), ellipsoid zone (EZ; originally called the inner/outer segment junction [13]) and/or interdigitation zone (IDZ; also called the cone outer segment tips [14]) were disrupted at the retinal areas of visual field defects in eyes with the AZOOR-complex [15–24]. It was also reported that the abnormalities in the outer retinal microstructures can recover during the follow-up period in some patients with the AZOOR-complex [18–20,22]. However, there has not a study that analyzed how these three highly reflective bands change with time during a fixed time period for many patients.

Therefore, the purpose of this study was to determine by SD-OCT the changes in the outer retinal microstructures during a six month period after the initial visit in eyes with AZOOR-complex.

Subjects and Methods

Subjects

We reviewed the medical records of patients who were diagnosed with AZOOR-complex who visited the Mie University Hospital or the Nagoya University Hospital from September 2007 to June 2013. Because the purpose of this study was to determine the changes of the retinal microstructures at the early stages of AZOOR-complex, only the patients whose initial examination was ≤3 months from the onset were studied. In addition, only the patients who were followed for at least six months after the initial visit were included. Based on these criteria, seventeen eyes of 17 patients with the AZOOR-complex were studied.

All patients had undergone a complete eye examination including best-corrected visual acuity (BCVA) measured by a standard Japanese decimal visual acuity chart at 5 m, slit-lamp biomicroscopy, color fundus photography, Humphrey static perimetry (30-2 program), and SD-OCT. Fluorescein angiography was performed only at the initial visit. Full-field electroretinograms (ERGs) or multifocal ERGs were recorded at the initial visit for a correct diagnosis of the AZOOR-complex [2,3].

The procedures used conformed to the tenets of the World Medical Association's Declaration of Helsinki. Mie University Institutional Ethics Review Board approved this retrospective study of the patients' medical records. Written informed consent was not given by participants for their clinical records to be used in this study, but patient information was anonymized and de-identified prior to analysis.

Spectral-domain optical coherence tomography (SD-OCT)

All of the patients had undergone SD-OCT examinations with the Spectralis OCT (HRA+OCT, Heidelberg Engineering) or the Cirrus HD-OCT (version 5.1, Carl Zeiss Meditec). Following the dilation of the pupils, the retinal tomographic images of 9 mm (approximately 30°) horizontal scans for Spectralis or horizontal 6 mm scans for Cirrus were obtained across the fovea. Depending on the image quality, B-scans were averaged.

We evaluated the SD-OCT findings at the initial visit and at six months. The reason why we selected the SD-OCT findings at 6 months was because Gass et al. [4] had reported that the alterations of the patients' vision stabilized within six months of the onset in 77% of the patients. We evaluated the integrity of the three highly reflective bands at the outer retina obtained by the SD-OCT; the external limiting membrane (ELM), ellipsoid zone (EZ) [13], and interdigitation zone (IDZ) [14]. The integrity of these bands was divided into three types; "continuous", "discontinuous", or "absent". The bands were defined as "continuous" when they were seen clearly and appeared to be continuous. The bands were defined as being "discontinuous" when they were blurred or interrupted. The bands were defined as "absent" when they were not identified at the area of the visual field defect. These decisions were made by two retinal specialists (YM and HM) independently and were masked to the other clinical findings. In addition, the preservation of outer nuclear layer (ONL) was also assessed.

To evaluate the changes in the outer retinal highly reflective bands more quantitatively, a longitudinal reflectivity profile (LRP) was created by previously described methods [13,25,26]. In brief, one vertical straight line was drawn at the retinal area of the visual field defect. The LRPs were made by calculating median values of pixels across each level of 20 adjacent A-scans using ImageJ (National Institutes of Health, Bethesda, MA; available at rsbweb.nih.gov/ij/download.html).

Results

The clinical characteristics and SD-OCT findings of the 17 Japanese patients with AZOOR-complex (three men and 14 women; age, 19–49 years) are summarized in Table 1. The diagnosis of our 17 patients included 10 with AZOOR, 4 with MEWDS, and 3 with AIBSE. The average interval between the onset of symptoms and examination in our hospital was 3.6 weeks with a range of 1 to 12 weeks. The average spherical equivalent refractive error was -4.4 diopters (D) with a range of -0.5 to -13.5 D. The type of visual field defects included two with a central scotoma, six with a paracentral scotoma, two with a temporal scotoma, and seven with a centro-temporal scotoma (Table 1).

Case Presentations

Case 11: MEWDS Associated with ONL Loss. A 35-year-old myopic woman presented with complaints of acute vision reduction and photopsia in her right eye. Her best-corrected visual acuity (BCVA) was 0.5 OD, and perimetry showed a visual field defect within 30 degrees of the fovea (Fig. 1A). Fundus examination showed multiple small, gray-white patches at the level of RPE and outer retina in the mid-peripheral region, and these white patches disappeared within four weeks without treatment. Based on these clinical findings, she was diagnosed with MEWDS. She was followed up without any treatments.

Her SD-OCT findings at the initial visit are shown in Figures 1B and 1C. In the central retinal area where the ONL was intact (yellow dotted square, Fig. 1B), the ELM was judged to be "discontinuous", and the EZ and IDZ were classified as being "absent". This was because these two lines were merged with the RPE-Bruch's membrane complex and were not identified as independent bands (Fig. 1C).

At six months after the initial visit, the decimal BCVA had improved to 1.2, and the visual field had recovered at many points (Fig. 1D). SD-OCT also showed an improvement in the outer retinal microstructures but only at the area of the intact ONL (yellow dotted square, Figs. 1E and 1F). At this time, the ELM and EZ were judged as "continuous", but the IDZ was still judged as "discontinuous" at the central area.

We also noted that this patient had an area of the retina where the ONL was completely absent at the initial visit (red square, Fig. 1B), and there was no recovery of the both the visual field and the SD-OCT image in this area at 6 months (red square, Fig. 1E).

Case 1: AZOOR with Recovery of Outer Retinal Microstructures. A 30-year-old emmetropic woman had an acute onset of photopsia and vision reduction in her right eye. Her decimal BCVA was 1.0 OD, and fundus examination and fluorescein angiography were essentially normal. However, perimetry showed severely decreased retinal sensitivities within 20 degrees of the fovea in the right eye (Fig. 2A). Multifocal ERGs also showed reduced focal ERGs within 20 degrees of the fovea. Based on these findings, this patient was diagnosed with AZOOR. She was followed without any treatments.

Her SD-OCT findings at the initial visit are shown in Figures 2B and 2C. The ELM and EZ were judged to be "discontinuous", because they were disrupted away from the macula (Figs. 2B and 2C). The IDZ was judged to be "absent" because this band was not identified over the entire 9 mm scan.

Table 1. Clinical Characteristics and SD-OCT findings of Patients with AZOOR-Complex.

Case/Sex/Age (y)/Eye	Diagnosis	Initial visit from the onset (week)	Spherical equivalent refractive error (dioptor)	Type of Scotoma	BCVA initial/6M	ELM initial/6M	EZ initial/6M	IDZ initial/6M	Improvement in visual field
1/F/30/Right	AZOOR	2	−0.5	Paracentral	1.0/1.2	II/I	II/I	III/II	Significant
2/M/35/Right	AZOOR	4	−0.5	Paracentral	1.2/1.5	I/I	I/I	II/I	Significant
3/F/34/Right	AZOOR	1	−11.5	Centro-temporal	0.5/0.7	II/II	III/III	III/III	None
4/F/19/Right	AZOOR	2	−3.0	Temporal	0.9/1.2	II/I	II/I	III/III	Mild
5/F/49/Left	AZOOR	12	−13.5	Centro-temporal	0.8/0.6	III/III	III/III	III/III	None
6/F/30/Right	AZOOR	4	−7.0	Centro-temporal	0.5/0.8	I/I	II/I	II/III	Mild
7/F/37/Left	AZOOR	1	−8.5	Centro-temporal	0.6/1.0	II/I	II/I	III/III	Mild
8/F/25/Left	AZOOR	8	−6.6	Centro-temporal	0.2/0.8	I/I	II/I	III/III	Mild
9/M/42/Right	AZOOR	2	−6.0	Paracentral	1.2/1.2	I/I	II/I	III/I	Mild
10/F/19/Right	AZOOR	1	−4.5	Centro-temporal	0.6/1.2	II/II	II/I	III/I	Significant
11/F/35/Right	MEWDS	2	−10.0	Central	0.5/1.2	II/I	III/I	III/I	Significant
12/F/31/Left	MEWDS	1	−6.5	Central	0.3/1.2	II/I	II/I	III/I	Significant
13/M/39/Right	MEWDS	8	−0.5	Centro-temporal	0.2/1.2	II/I	III/I	III/I	Significant
14/F/24/Right	MEWDS	1	−2.75	Paracentral	0.8/1.2	II/I	II/I	III/I	Significant
15/F/47/Right	AIBSE	1	−2.0	Temporal	1.2/1.2	I/I	II/I	III/III	None
16/F/37/Left	AIBES	3	−0.5	Paracentral	1.2/1.0	II/I	II/I	III/I	Significant
17/F/29/Left	AIBSE	8	−5.75	Paracentral	1.0/1.2	I/I	II/I	III/I	Significant

Abbreviations: AZOOR, acute zonal occult outer retinopathy; MEWDS, multiple evanescent white dot syndrome; AIBSE, acute idiopathic blind spot enlargement; BCVA, best-corrected visual acuity; ELM, external limiting membrane; EZ, ellipsoid zone; IDZ, interdigitation zone; I, continuous; II, discontinuous; III, absent.
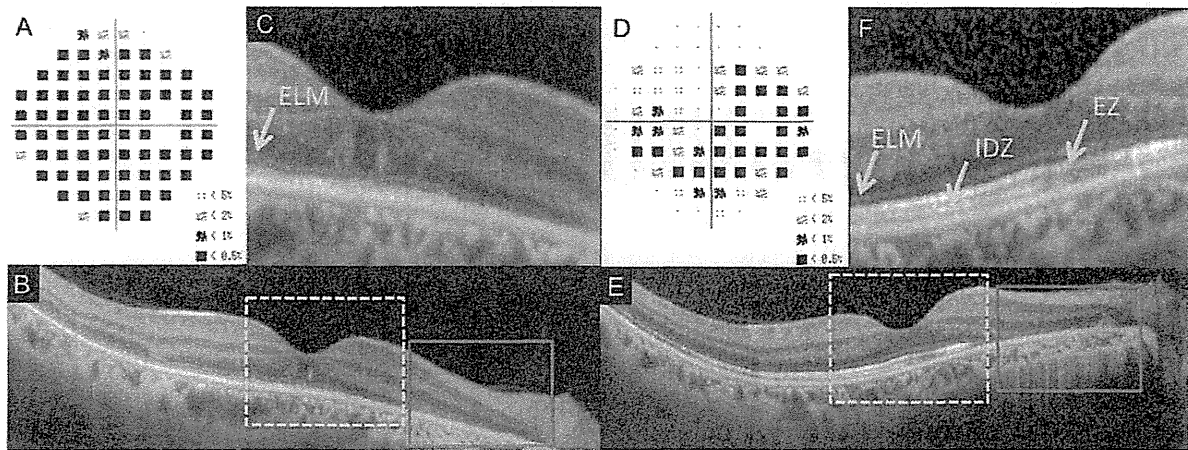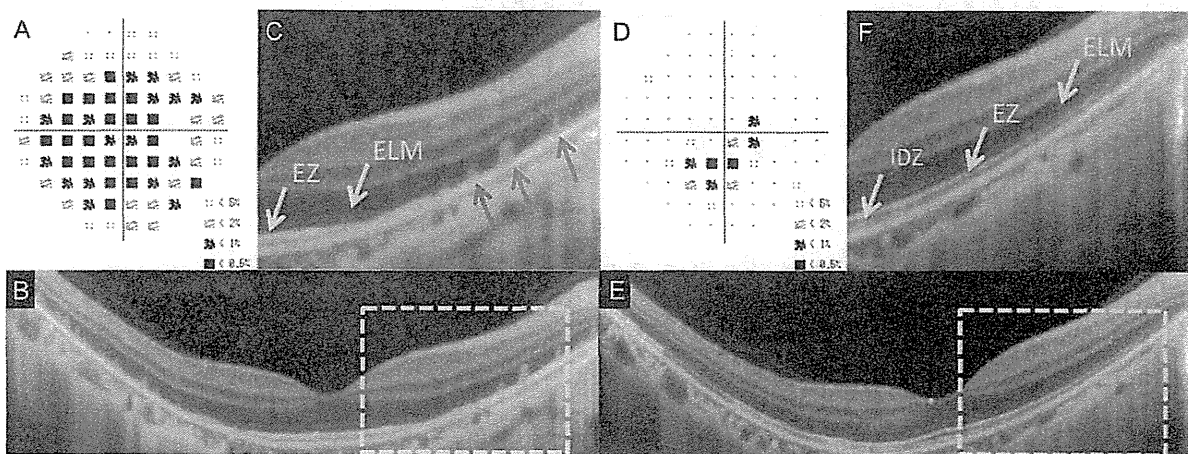
Figure 1. Static visual field and spectral-domain optical coherence tomographic (SD-OCT) results of the right eye of Case 11 at the initial visit (A–C) and six months after the initial visit (D–F). A: Deviation plot obtained by the Humphrey 30-2 program at the initial visit. B: Horizontal SD-OCT image through the fovea at the initial visit. C: Magnified view of the area outlined by dashed yellow line box in the image of B. D: Deviation plot obtained with the Humphrey 30-2 program at six months after the initial visit. E: Horizontal SD-OCT image through the fovea at six months after the initial visit. F: Magnified view of the area outlined by dashed yellow line box in the image of E. ELM, external limiting membrane. EZ, ellipsoid zone. IDZ, interdigitation zone. This case had the retinal area where the outer nuclear layer (ONL) was completely absent (red line boxes).
doi:10.1371/journal.pone.0110592.g001

Interestingly, the retina had highly reflective materials in columns which passed through the ONL from the RPE at the area of visual field defect (red arrows, Fig. 2C). Similar highly reflective materials have been reported in a patient with MEWDS [20].

After six months, there was a marked improvement in her visual fields (Fig. 2D), and SD-OCT showed a recovery of the outer retinal microstructures. At this time, the ELM and EZ were judged to be "continuous". However, the IDZ was still "discontinuous", because it was only identified in the central area (Figs. 2E and 2F). We also noticed that the columnar highly reflective materials were

not present at six months. The ONL was preserved in the initial and 6 months SD-OCT images.

Case 2: AZOOR with Intact EZ at Initial Visit. A 35-year-old healthy emmetropic man reported that he had an acute paracentral visual field depression and photopsia in his right eye. His decimal BCVA was 1.2 OD. His fundus and fluorescein angiography were normal, but visual field showed extensive defects outside the fovea in the right eye (Fig. 3A). His scotopic and photopic full-field ERGs were reduced but only in the right eye.

Figure 2. Static visual field and spectral-domain optical coherence tomography (SD-OCT) results of the right eye of Case 1 at the initial visit (A–C) and six months after the initial visit (D–F). A: Deviation plot obtained with the Humphrey 30-2 program at the initial visit. B: Horizontal SD-OCT image through the fovea at the initial visit. C: Magnified view of the area outlined by dashed yellow line box in B. D: Deviation plot obtained with the Humphrey 30-2 program at six months after the initial visit. E: Horizontal SD-OCT image through the fovea at six months after the initial visit. F: Magnified view of the area outlined by dashed yellow line box in the image of B. ELM, external limiting membrane. EZ, ellipsoid zone. IDZ, interdigitation zone. Several column-shaped highly reflective materials are seen at the outer retinal area of visual field defect at the initial visit (red arrows).
doi:10.1371/journal.pone.0110592.g002